# Green Chemistry

Accepted Manuscript






ROYAL SOCIETY OF CHEMISTRY

www.rsc.org/greenchem

Journal Name

ARTICLE

# Catalytic Transfer Hydrogenation of Ethyl Levulinate to γ-Valerolactone over Zirconium-based Metal-Organic Frameworks

Received 00th January 20xx,
Accepted 00th January 20xx

DOI: 10.1039/x0xx00000x

www.rsc.org/

**Anil H. Valekar,[a,c] Kyung-Ho Cho,[a] Sachin. K. Chitale,[a,c] Do-Young Hong,[a,c] Ga-Young Cha,[a,c] U-Hwang Lee,[a,c] Dong Won Hwang,[a,c] Christian Serre,[d] Jong-San Chang*[a,b] and Young Kyu Hwang*[a,c]**

A series of highly crystalline, porous, zirconium-based metal-organic frameworks (Zr-MOFs) with different ligand functionality and porosity were applied for catalytic transfer hydrogenation of ethyl levulinate (EL) to form γ–valerolactone (GVL), using isopropanol as a hydrogen donor. The role of ligand functionality and the metal center of the Zr-MOFs were identified and reaction parameters were optimized, for selective production of GVL. Maximum yield of GVL (up to 92.7%) was achieved in 2 h at 200°C with UiO-66(Zr). Interestingly, zirconium trimesate (MOF-808) emerged as the most suitable candidate, with the highest GVL formation rate (94.4 μmol/g/min) among the catalysts tested at 130°C. It was also found effective in conversion of EL to GVL in an open system using the solvent refluxing method. Both the catalysts (UiO-66(Zr) and MOF-808) were recycled at least five times under their specified reaction conditions without notable change in catalytic activity and product selectivity. Fresh and recycled catalysts were characterized in detail using X-ray diffraction (XRD), $N_2$ adsorption-desorption, thermal gravimetric analysis (TGA), Fourier transform infrared spectroscopy (FTIR) and scanning electron microscopy (SEM) in order to understand the stability and structural changes that occurred in the catalysts. Finally, a plausible reaction mechanism was presented on the basis of active sites present in catalysts confirmed by characterization results.

## 1. Introduction

The growing demand for energy to improve the quality of life and the gradual depletion of fossil resources along with environmental deterioration, have left researchers in a quest for alternative renewable resources. Among several renewable resources, only biomass some of which is inexpensive and abundant in nature is a sustainable source of liquid fuels and chemicals otherwise conventionally derived from fossil resources.[1, 2] Enormous efforts are being made to develop suitable catalytic processes for the production of various platforms and value-added chemicals from carbohydrate, or directly from lignocellulosic biomass.[3-11] Among these chemicals, γ-Valerolactone (GVL) is recognized as a versatile building block that could be utilized as an additive in liquid fuel for transportation,[12, 13] as precursor for the production of polymeric monomers, [14, 15] and for creation of various value-added chemicals including organic solvents and bio-oxygenates.[16, 17] GVL itself has proved an excellent green solvent for biomass processing due to its extraordinary physicochemical properties, which include low melting and high boiling points; remarkably low vapor pressure, even at elevated temperature and its ready miscibility with water without forming an azeotropic mixture.[18-20]

Generally, three major strategies have been explored for GVL production from levulinic acid (LA) and its ester, based on diversity of the hydrogen source.[21] Molecular $H_2$ is the most common hydrogen source used for this reaction, which occur in the presence of various metal catalysts (e.g., Ru, Pt, Pd, Ni, Co, Cu, Rh, Re and Mo).[22-28] Formic acid (FA), which forms in equimolar amount with LA during acid hydrolysis of carbohydrates, is also utilized as a hydrogen source to produce GVL from LA to embodies the principle of atom economy. Several catalytic systems including RuRe/C, Au/$ZrO_2$-VS, ruthenium immobilized functionalized silica, nickel promoted copper-silica and Ag-Ni-$ZrO_2$ nanocomposites have been successfully utilized for quantitative conversion of LA into GVL, while consuming equimolar FA as a hydrogen donor.[29-33] However, both the hydrogenation strategies mentioned above have some limitations (e.g.., harsh reaction conditions, use of corrosive acids, use of precious metals and non-environmental friendly solvents) that restrict their large scale application to a certain extent.[34]

Recently, Dumesic *et al.* reported for the first time, a catalytic transfer hydrogenation (CTH) method based on the principle of Meerwein-Ponndorf-Verley (MPV) reduction for the hydrogenation of LA and alkyl levulinates to GVL over heterogeneous catalysts using secondary alcohols as hydrogen donor. They demonstrated that $ZrO_2$ displayed better activity than the other metal oxides tested due to its amphoteric nature.[35] The high chemical selectivity of MPV reduction toward the carbonyl groups of aldehyde and ketones, replacement of molecular $H_2$ by alcohols, and effective performance of catalysts comprising non-precious metals provide a

[a] Research Center for Nanocatalysts, Korea Research Institute of Chemical Technology, Daejeon 305-600, Korea E-mail:jschang@krict.re.kr ykhwang@krict.re.kr
[b] Departments of Chemistry, Sungkyunkwan University, Suwon 440-476, Korea
[c] Department of Green Chemistry and Environmental Biotechnology, University of Science and Technology (UST),217 Gajeong-Ro, Yuseong, Daejeon 305-350, Korea
[d] Institut Lavoisier, UMR CNRS 8180, Université de Versailles St-Quentin en Yvelines, 45 Avenue des Etats-Unis,78035 Versailles Cedex, France
† Footnotes relating to the title and/or authors should appear here.
Electronic Supplementary Information (ESI) available: [details of any supplementary information available should be included here]. See DOI: 10.1039/x0xx00000x

cost-effective alternative for the production of GVL. Therefore, within a short period of time, a variety of catalytic systems mainly based on zirconium such as $ZrO_2$[36], $ZrO(OH)_2$[37], Al-Zr mixed oxides[38] and amorphous Zr-complexes [zirconium 4-hydroxybenzoate (Zr-HBA),[34] zirconium phosphonate (Zr-PhyA)[39]] have been reported for this reaction. Very recently, GVL was produced via vapor phase and microwave assisted systems over $ZrO_2$/SBA-15[40] and Ru/C[41], respectively. In the category of crystalline porous material, several zeolites such as Zr-Beta, Ti-Beta, Sn-Beta, Al-Beta and Al-MFI-ns were tested for GVL production from LA and its ester. [42,43] Moreover, Linh Bui et al. used Brönsted and Lewis acid zeolite mixture for selective production of GVL directly from furfural.[43]

Metal-organic frameworks consist of metal nodes or clusters, bridged through organic ligands to form a well ordered, and highly crystalline porous network. Its exceptional properties such as large surface area, tunable pore size, coordinatively unsaturated sites (CUSs), and functionality of metal ions and organic ligands provide additional advantages in catalysis over non-porous and zeolitic materials.[44-46] From the point of view of catalysis, the high surface area and permanent porosity of MOFs, accessible through continuous and permeable channels, can provide a greater number of active sites for the reactant. The presence of larger channels or cages further facilitates diffusion, which enhances the interaction between reactant and the active sites present in the porous network. Subsequently, the rate of reaction and turn over frequency (TOF) increases, which is highly desirable from the perspective of green chemistry. Nevertheless, the relatively lower hydrolytic and thermal stability of various MOFs, compared to zeolite restricted its practical applications in various fields.[47, 48] Fortunately, Zr-MOFs exhibit unprecedented chemical, thermal, and mechanical stability due to higher co-ordination number of Zr in the framework.[49, 50] Recently, several authors explored this material for a variety of applications such as gas and water adsorption, separation, sensing and catalysis.[51-55]

In this work, a series of zirconium MOFs were selected to study the CTH of EL to GVL using isopropanol as H-donor. Isopropanol has already been proven as the preeminent H-donor alcohol due to its low reduction potential.[37] We preferred EL as feedstock over LA considering as a model compound which possibly would not block the basic sites of catalyst as LA does.[35] In addition, there are no safety and economical concern over corrosion of reactors because of its acid free form. To the best of our knowledge, no report has been focused on GVL formation from LA or its ester using porous crystalline metal-organic frameworks (MOFs) prior to this article. In our study, we have explored the role of the metal center, ligand functionality, and porous properties of Zr-MOFs for the conversion of EL and selective formation of GVL. Effect of different process parameters on the selectivity of products was investigated and a plausible reaction mechanism was proposed based on findings of active centers present in the MOFs. Detailed characterizations of fresh and used catalysts were conducted to check their stability and structural changes the under applied reaction conditions.

## 2. Experimental

### 2.1 Chemicals and materials

Ethyl levulinate (99%), γ-valerolactone (99%), 2-propanol (99.5%), naphthalene (98%), $ZrOCl_2.8H_2O$ (98%), $ZrCl_4$ (99.5%), 1,4-benzenedicarboxylic acid ($H_2BDC$, 98%), 1,2,4-benzenetricarboxylic acid ($H_3BTC$, 99%), 2-aminoterphthalic acid (99%), 1,3,5-benzenetricarboxylic acid ($H_3BTC$, 95%), benzoic acid (99.5%), acetic acid (99.7%), hydrochloric acid (HCl, 37%) and N,N-dimethylformamide (99.8%) were obtained from Sigma-Aldrich. Formic acid (99%) and fumaric acid (99%) were purchased from Samchun Pure Chemicals (South Korea) and iosopropyl 4-oxovalerate (95%) was supplied by Beta Pharma Co. Ltd. (Shanghai, China). All the chemicals were used without further purification.

### 2.2 Catalyst preparation

*Synthesis of UiO-66(Zr) and its functionalized analogs:*

UiO-66(Zr) synthesis was carried out by reflux method.[56] Typically, 4.62 g (27.8 mmol) of $H_2BDC$ was initially dissolved in DMF (23.6 g, 322 mmol) at room temperature in a 100 ml round flask. Then, 8.96 g (27.8 mmol) of $ZrOCl_2{\cdot}8H_2O$ and 4.63 mL of 37% HCl (5.47 g, 150 mmol) were added to the mixture. The molar ratio of the final $ZrOCl_2{\cdot}8H_2O/H_2BDC/DMF/HCl$ mixture was 1:1:11.6:5.4. The reaction mixture was vigorously stirred to obtain a homogeneous gel. The mixture was then heated to 150°C and kept at this temperature for 6 h, leading to a crystalline UiO-66(Zr) solid. The resulting product was recovered from the slurry by filtration, re-dispersed in DMF at 60°C for 6 h while stirring, and then recovered by filtration. The same procedure was repeated twice, using MeOH instead of DMF. The solid product was finally dried at overnight 100°C.

UiO-66(Zr)-$NH_2$ was synthesized by the reflux method. Initially, 1.94g of 2-amino- terphthalic acid (10.7 mmol) was dissolved in 38.4 ml $H_2O$ and 9.2 ml acetic acid (160.1 mmol) solution in a 100 ml round flask. Then, 3.44 g of $ZrOCl_2{\cdot}8H_2O$ (10.7 mmol) was added to the solution with continuous stirring. The molar ratio of the final $ZrOCl_2{\cdot}8H_2O/H_2BDC\text{-}NH_2/H_2O/CH_3COOH$ mixture was 1:1:200:15. The reaction solution was ramped to 100°C and kept for 24 h. After cooling to room temperature, the precipitate in the reaction solution was filtered. To remove the residual precursor and ligands, the precipitates were sufficiently washed with water and ethanol at 80°C and 60°C, respectively. Finally, the product was dried overnight at 100°C.

UiO-66(Zr)-COOH was also synthesized using the reflux method. Briefly, 14g of 1,2,4-benzenetricarboxylic acid (66.7 mmol) and 10.74 g of $ZrOCl_2{\cdot}8H_2O$ (33.3 mmol) were dissolved in a solution of 30 ml $H_2O$ and 20.4g of benzoic acid (166.6 mmol) in a 100ml round flask. The molar ratio of the final $ZrOCl_2{\cdot}8H_2O/H_3BTC/H_2O/C_6H_5COOH$ mixture was 1:2:50:5. Then, the reaction solution was ramp to 100°C and kept for 24 h. Work-up was done exactly the same way mentioned in the procedure used above for UiO-66(Zr)-$NH_2$.

*Synthesis of MOF-808:* $H_3BTC$ (4.8 g, 0.5 mmol) and $ZrOCl_2{\cdot}8H_2O$ (3.3 g, 0.5 mmol) were added to a solvent mixture of DMF/formic acid (270 mL/360 mL). Reaction mixture was transferred to a 1L Teflon-lined pressure autoclave and heated at 135°C for two days. White precipitate was collected by centrifugation and washed with DMF (24 h), followed by ethanol (24 h). The respective solvents



 

were replaced twice during that period. Finally, the product was dried at 100°C for 12 h.

*Synthesis of MOF- 801*: MOF-801, commonly known as Zr-Fumarate MOF, has been synthesized according to the procedure published earlier.[57] Briefly, $ZrCl_4$ (2.585 mmol, 1 eq) was dissolved in 50 ml water. Then, formic acid (258.5 mmol, 100 eq) as a modulator and fumaric acid (7.75 mmol, 3 eq) as a linker molecule was added to the solution of the metal precursor. The reaction mixture transferred into a Teflon-lined pressure vessel and heated at 120°C for 24 h. White precipitate was collected by centrifugation and washed with ample water and ethanol. Finally, the product was dried at overnight 100°C.

*Synthesis of $ZrO(OH)_2$ and $ZrO_2$:* Zirconium oxyhydroxide were synthesized as reported elsewhere.[37] Concentrated $NH_4OH$ was added into aqueous solution (100 g/L) of $ZrOCl_2{\cdot}8H_2O$ with vigorous stirring to adjust the solution pH in between 9 to 10. Resulting emulsion was aged for 24 h, filtered and then thoroughly washed with water. Solid precipitate dried at 100°C overnight to get $ZrO(OH)_2$. $ZrO_2$ was prepared by calcination of $ZrO(OH)_2$ at 500°C for 5 h in air.

### 2.3 Catalyst characterization

Powder diffraction patterns were obtained by Rigaku diffractometer using Ni-filtered Cu Kα- radiation (40 kV, 30 mA, λ=1.5406 Å). The $N_2$ adsorption-desorption isotherms were measured at 77 K using a Micromeritics Tristar 3000. The samples were dehydrated under vacuum at 423 K for 12 h prior to analysis. The specific surface areas were evaluated using the Brunauer-Emmett-Teller (BET) method and the pore volume was determined by the single point method at $p/p_0$ = 0.99. The micropore size distribution was determined from Ar sorption techniques using the Horvath-Kawazoe method. Thermal gravimetric analysis (TGA) of the catalysts was performed on a Sinco TGA-N 1000 thermal analyzer. The samples were run at a heating rate of 5°C/min in the range of 25 to 700°C under constant flow of nitrogen at 20 ml/min. FTIR spectra were recorded on a Nicolet FTIR spectrometer (MAGNA-IR 560) using KBr pellets. Morphological properties of the catalysts were studied by scanning electron microscopy (SEM) (Tescan Mira 3 LMU FEG with accelerating voltage of 10 kV). Acidic and basic properties of the catalysts were measured using $NH_3$-TPD and $CO_2$-TPD, respectively. TPD profiles of catalysts were measured on a Micromeritics AutoChem II 2920 V3.05 apparatus equipped with a thermal conductivity detector. Samples were activated at 150°C for 12h in a helium flow, prior to the adsorption step. Subsequently, activated samples were exposed to $NH_3$ or $CO_2$ gases at 50°C for 30 minute with a flow rate of 50 mL/min. Initially, physically adsorbed $NH_3$ or $CO_2$ gases were removed by purging with helium gas for 1 h at the same temperature and flow rate. TPD data were recorded from 50°C to 300°C with heating rate of 5°C/min. Inductively coupled plasma (ICP) analysis was used to determine the metal leaching from the Zr-MOFs. Elemental analysis (EA) was performed to determine the carbon and hydrogen content in the catalyst.

### 2.4 Catalytic test and product analysis

In a typical run, 4 mmol of EL, 400 mmol of 2-propanol, 0.24g of naphthalene as an internal standard and respective amounts of catalyst were filled to a 100 mL stainless steel reactor containing an inner lining of Pyrex glass and equipped with magnetic stirrer. The reaction was conducted at a certain known temperature for the desired time. Catalyst was separated by filtration and washed thoroughly with ethanol-water system (95:5). The filtrate were subjected to quantitative analysis using gas chromatography (GC, FID detector and HP-5 column) and identification of the products was done by GC-MS (Agilent 6890N GC and 5973 N MSD). For the open-system solvent-reflux method, reactions were carried out in two-neck, 50 mL round-bottom flasks equipped with septum ports and reflux condensers. EL conversion and yield of products were defined using the following equations shown in eqn. (1) and (2).

$$EL\ conversion\ (\%) = (1 - \frac{mole\ of\ EL}{Initial\ mole\ of\ EL})\ X\ 100) \quad \ldots\ldots\ldots (1)$$

$$Product\ yield(\%) = (\frac{mole\ of\ product}{Initial\ mole\ of\ EL})\ X\ 100 \quad \ldots\ldots\ldots\ldots\ldots\ldots (2)$$

## 3. Results and discussions

The MPV reduction reaction for different substrates can be effectively catalyzed by several Zr-containing catalysts, including porous and non-porous materials such as metal oxides, [35, 36] metal hydroxides, [37] amorphous metal complexes [34, 39] and zeolites.[42, 43] Owing to the potential of porous materials for MPV reduction reaction, various zirconium-based metal-organic frameworks (Zr-MOFs) were tested for CTH of EL to GVL as shown in **Scheme 1**

### 3.1 Role of metal center/cluster and ligand functionality of Zr-MOFs in CTH of EL

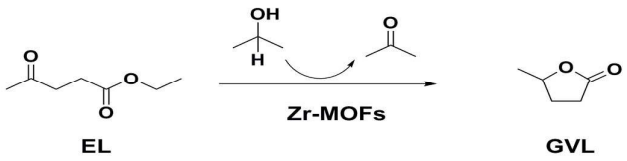


**Scheme 1** Catalytic transfer hydrogenation of EL to GVL using Zr-MOFs

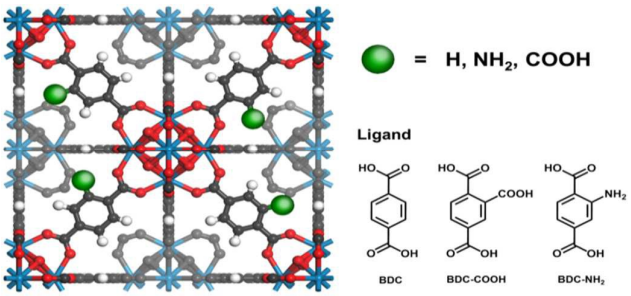


**Fig. 1** Representative structure of UiO-66(Zr) and its functionalized analogs with different ligands.

**Table 1** Physico-chemical properties and catalytic activity of UiO-66(Zr) and its functionalized analogs in CTH of EL to GVL

| Entry | Catalysts | $S_{BET}$ [b] ($m^2/g$) | PV [c] ($cm^3/g$) | Conv.[d] (%) | $Y_{GVL}$ [e] (%) | $Y_{IPL}$ [f] (%) |
|---|---|---|---|---|---|---|
| 1 | None | ---- | ---- | 8.9 | 2.7 | 1.0 |
| 2 | UiO-66(Zr) | 1046 | 1.65 | 100 | 53.5 | 44.2 |
| 3 | UiO-6(Zr)-COOH | 575 | 0.80 | 28.5 | 13.9 | 13.5 |
| 4 | UiO-6(Zr)-$NH_2$ | 1006 | 1.8 | 97.6 | 27.3 | 64.6 |

[a] Reaction conditions: EL 4 mmol, isopropanol 400 mmol; catalyst 0.8 g; naphthalene 0.24g; temperature 150°C; time 4 h. [b] $S_{BET}$ = BET surface area as a nominal surface area, [c] PV = Pore Volume, [d] Conv. = Conversion, [e] $Y_{GVL}$ = GVL yield and [f] $Y_{IPL}$= Yield of isopropyl levulinate (IPL).

MOFs possess multifunctional properties derived both from a metal cluster and ligand functionality. Therefore, it is highly desirable to understand the origin of active centers (either of metal cluster or ligand), to design a material superior for the respective applications. Considering this point, we synthesized UiO-66(Zr) and its functionalized analogs distinguished on the basis of ligand functionality, as shown in **Fig. 1**. Their structures were confirmed using XRD, FTIR, $N_2$ adsorption and TG analysis; and are reported in the supplementary information **(Fig.S1)**. The obtained results were well matched with earlier reports.[58, 59, 60]

The physicochemical properties and catalytic activity of UiO-66(Zr) and its functionalized analogs with acid (COOH) and base ($NH_2$) group in the framework of the ligand are summarized in **Table 1**. UiO-66(Zr) catalyst has a large BET surface area (1046 $m^2/g$) and pore volume (1.65 $cm^3/g$). Replacement of the BDC ligand by electron donating and withdrawing groups functionalized BDC, significantly altered its chemical and physical properties. The presence of carboxylic acid functionality in the ligand delivers extra acidity to the UiO-66(Zr) framework. However, considerable loss in surface area and pore volume of UiO-66(Zr)-COOH was observed, probably due to partial consumption of available space in the pores by free carboxylic groups. In contrast, the presence of amino groups in the ligand provides additional basicity to the UiO-66(Zr) structure with minor loss in surface area. This was ascribed to smaller size of $NH_2$ groups compared to COOH groups. Previous literature[61] and pore size distribution curves from Ar-physisorption **(Fig. S2)** shows that, the pore size of UiO-66(Zr) and its functionalized analogs increased in the order UiO-66(Zr)-COOH < UiO-66(Zr)-$NH_2$ < UiO-66(Zr).

Entry 1 in Table 1 shows that without catalyst, the reaction proceeded to a minor extent. Isopropyl levulinate (IPL), the transesterified product of EL, in the presence of 2-propanol, was the major side product observed in all cases. Among the tested catalysts, UiO-66(Zr), which has no ligand functionality, showed maximum EL conversion and GVL yield. Only 28.5% EL conversion and 13.9% GVL yield was achieved using UiO-66(Zr)-COOH catalyst. It should be noted that the low conversion was possibly due to the slow diffusion of EL into the narrow pores of UiO-66(Zr)-COOH or the reaction could be limited only to the external surface area of UiO-66(Zr)-COOH. On the other hand, nearly complete conversion of EL was observed using UiO-66(Zr)-$NH_2$. However, in product distribution, IPL was the major product with 64.6% yield. This clearly indicates that the transesterification reaction was predominant in presence of amine functionalized UiO-66(Zr). It has been reported that basic catalysts such as amine functionalized silicas [62, 63] and carbon nanotubes[64] are highly efficient in transesterification reactions. Furthermore, the presence of electron donating or withdrawing groups on ligands can change the charges on metal cluster which significantly affects the catalytic activity. [65]

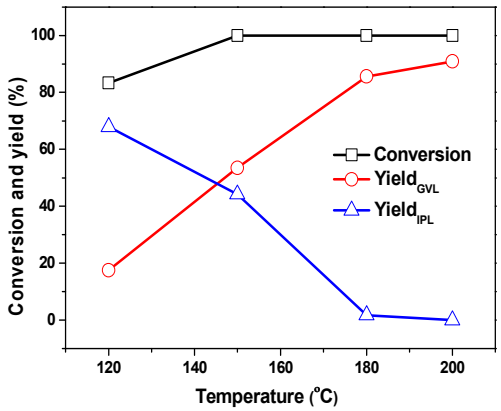


**Fig.2** Effect of reaction temperature in catalytic transfer hydrogenation of EL to GVL over UiO-66(Zr): Reaction conditions: EL 4 mmol, isopropanol 400 mmol, catalyst 0.8 g, naphthalene 0.24g, and reaction time 4 h.

This result indicated that large surface area, along with larger pore size, balanced acid-base property or charge on the metal cluster and easy access to the active center are the key factors in selective conversion of EL into GVL. Ligand functionality hampers the catalytic activity by changing electronic and the porous properties of the original UiO-66(Zr) framework.

### 3.2 Effect of reaction temperature and time.

The temperature dependence of this reaction was exhibited in the range 120 - 200°C for 4 h reaction time **(Fig.2)**. In most of the previous studies, transfer hydrogenation of LA or EL was carried out at moderate to high reaction temperature (120°C to 250°C).[34, 35, 36, 37, 39,] Furthermore, extraordinary thermal and chemical stability of UiO-66(Zr) was already been proved,[49, 66] which allowed us to extend the reaction temperature to 200°C. The reaction conversion was 83% at 120°C and reached to completion after increasing the temperature by 30 °C. Yield of GVL increased with reaction temperature and reached maximum to 92.7% at 200 °C. At the same time, the IPL yield decreased progressively with rise in reaction temperature from 67.9% at 120 °C to 0% at 200 °C. IPL is the major side product at lower reaction temperatures, most probably due to the presence of excess amount of isopropanol in reaction mixture. Metal center of UiO-66(Zr) in presence of excess isopropanol is likely to undergo transesterification reaction more rapidly to form IPL than CTH does to produce GVL. *Simultaneous*

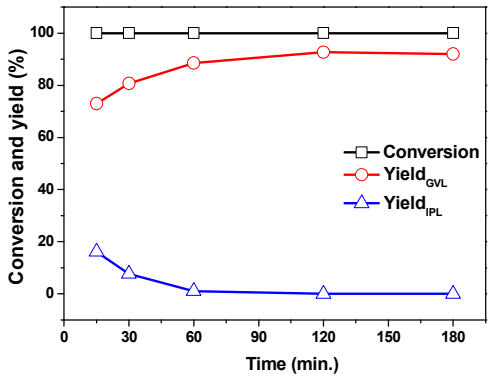


**Fig.3** Effect of reaction time in catalytic transfer hydrogenation of EL to GVL over UiO-66(Zr) : Reaction conditions: EL 4 mmol, isopropanol 400 mmol, catalyst 0.8 g, naphthalene 0.24 g, and reaction temperature 200$^{O}$C.

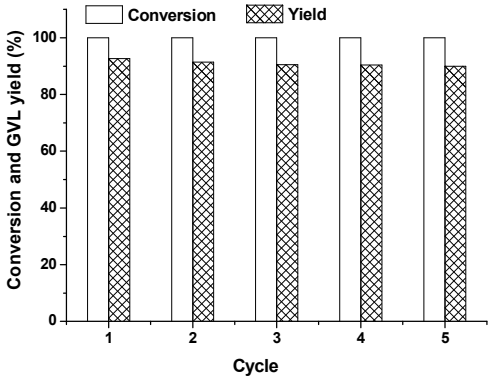


**Fig. 4** Recycle test of UiO-66(Zr) catalyst in catalytic transfer hydrogenation of EL to GVL: Reaction conditions: EL 4 mmol, isopropanol; 400 mmol, catalyst 0.8 g, naphthalene 0.24 g, reaction temperature 200$^{O}$C and reaction time 2 h.

*etherification and transfer hydrogenation reaction of oxygenates in presence of alcohol has been reported previously for Lewis acid zeolites.*[67] *Raising reaction temperature improved, GVL yield improved significantly* because IPL undergoes CTH as EL more effectively does at higher temperature. This observation concluded that GVL could be formed at lower temperature; however the rate of GVL formation increases with increasing reaction temperature.

We also examined the influence of reaction time on CTH of EL to GVL at 200$^{O}$C. Results show that, even at short duration (15 min) EL conversion reached completion **(Fig. 3)**. By increasing the reaction time from 15 to 120 min, GVL yield improved from 70 to 92.7%. Allowing the reaction continues for 3 h, did not change GVL yield. To the contrary, the IPL yield progressively declined with increasing reaction time. This observation supports that IPL can undergo MPV reaction as EL does, most likely with a lower reaction rate.

### 3.3 Catalyst recyclability and characterizations

A recycling test of UiO-66(Zr) for CTH of EL to GVL was studied under optimized reaction conditions, and the results are shown in **Fig. 4**. After every cycle, the catalyst was recovered by filtration, washed with an ethanol-water system (95:5) and dried prior to the next run. There was no marginal difference observed in the EL conversion and GVL yield, even after five cycles, indicating no loss of the active sites present in the catalyst.

In general, it is very difficult to predict the stability of MOFs under specific reaction conditions despite the high thermal stability provided by their chemical durability. Consequently, it is always necessary to check for changes in the crystalline structure, after reaction. Therefore, recycled UiO-66(Zr) catalyst was carefully studied using various characterization techniques, to confirm changes in its structural and morphological properties after five recycle tests **(Fig. 5)**. In the XRD patterns of used UIO-66(Zr), all peaks were preserved with little decrease in peak intensity, compared to fresh samples (Fig.5 a). Similarly, a negligible difference in BET surface area (1046 m$^2$/g and 1000 m$^2$/g) and pore volume (1.65 cm$^3$/g and 1.63 cm$^3$/g) of the catalyst was observed after five tests (Fig.5 b).

Nevertheless, differences in the TG curve of fresh and used catalysts were observed (Fig.5 c). Fresh catalyst absorbed more water than did the spent, which was determined by slightly greater weight loss before 75$^{O}$C and this was well supported by a small loss in BET surface area and pore volume of spent, compared to fresh, UiO-66(Zr). The number of BDC ligands present in the fresh and used UiO-66(Zr) was calculated from the weight loss that occurred in the temperature range of 350$^{O}$C to 550$^{O}$C. In spite of the good crystalline structure, fresh UiO-66(Zr) has one linker deficiency; this fact is in line with the results obtained in other studies where HCl was used as a deprotonating agent in the synthesis of UiO-66(Zr). [68, 69] Missing linker defects were assumed to be capped by the -OH groups. [69] In this case the proposed formula for fresh UiO-66(Zr) was $Zr_6O_4(OH)_4(OH)_2(BDC)_5$. After five cycles, the catalyst lost one more BDC linker from its framework (combining BDC anions with two protons from OH of a hexanuclear Zr cluster, and a departure of neutral acid) leaving a material with the formula $Zr_6O_6(OH)_4(BDC)_4$. The charge imbalance generated due to linker deficiency was compensated by partial replacement of $\mu_3$–$OH^-$ ions by $\mu_3$–$O^{2-}$ ions.[68] The stability of UiO-66(Zr) with two linker deficiency has also been reported previously.[68] FTIR analysis showed that the characteristic sharp peak at wavenumber 3673 cm$^{-1}$ assigned to bridged OH stretches [70, 71] in fresh catalyst, reduced considerably after recycle tests, which supported our hypothesis on charge balance. That the morphology of the catalyst remains unchanged was confirmed by SEM analysis **(Fig. S3)**.

ICP analysis did not detect any zirconium in the reaction filtrate. Additionally, higher Zr content was observed in the used catalyst than in the fresh catalyst. Contrarily, elemental analysis results show that carbon and hydrogen content decreased in the used catalyst (**Table S1).** This confirmed leaching of organic moiety, not of zirconium, from the MOF structure.

All the above observation reinforced the fact that, UiO-66(Zr) has a unique property in the ability to undergo structural rearrangement in ways that stabilize its structure. This unique property developed due to the high connectivity of zirconium in the

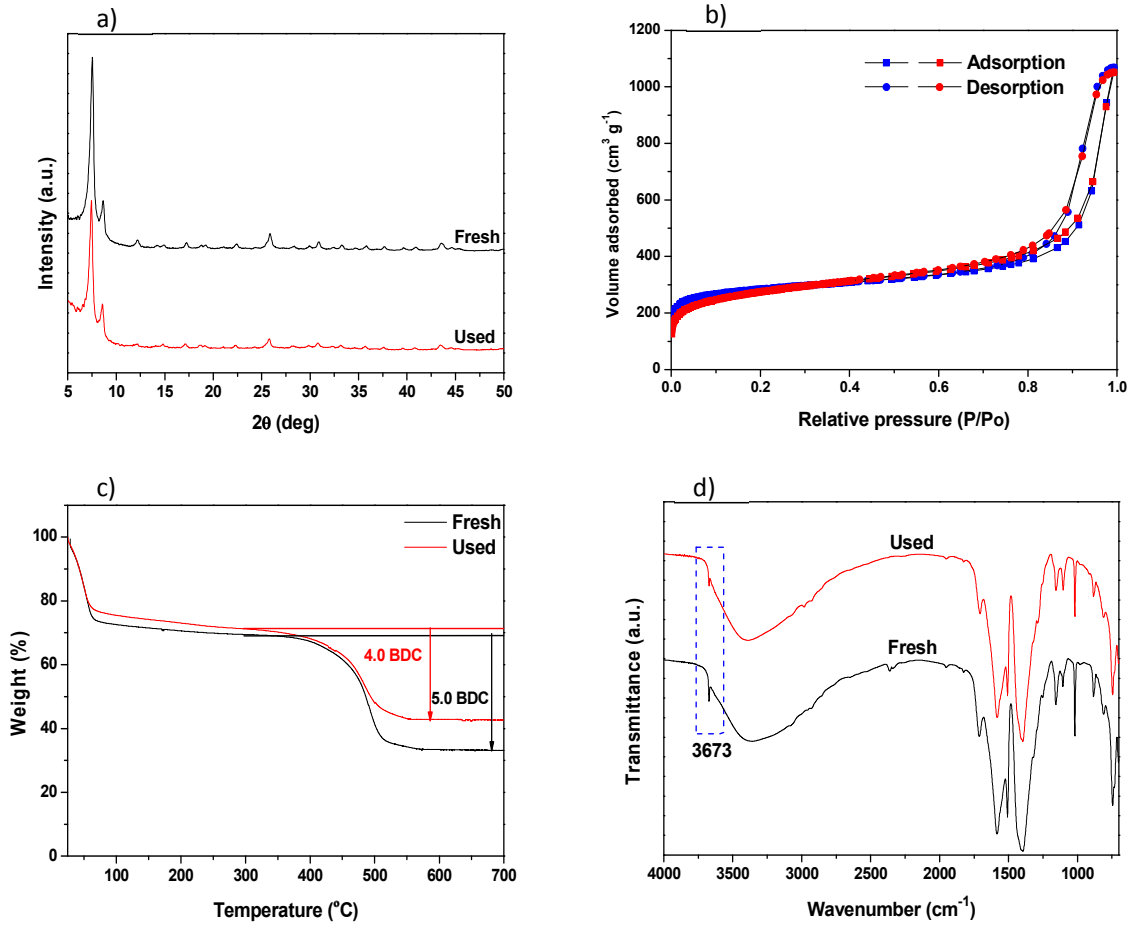


**Fig.5** Characterization of the fresh and used UiO-66(Zr) after 5 cycles: a) XRD pattern, b) $N_2$ adsorption-desorption isotherm at 77K , c) TGA curves, and d) FT-IR patterns.

UiO-66(Zr) framework. In spite of the structural rearrangement, the catalytic activity of UiO-66(Zr) was unaffected. This further Indicated that the metal nodes are the active sites, rather than the organic ligands in the selective transformation of EL to GVL.

### 3.4 Evaluation of Zr-MOFs possessing different physico-chemical properties for CTH of EL to GVL

After confirming the active sites in UiO-66(Zr) for transfer hydrogenation of EL, we planned to check the possibility that of other Zr-MOFs might be more suitable candidates for this reaction. To overcome the use of high reaction temperature was another issue behind this objective. For this purpose, two alternative Zr-MOFs (MOF-801 and MOF-808), which possesses metal center ($Zr_6O_4(OH)_4$) in their framework like UiO-66(Zr) were selected for this reaction. **Table 2** represents the porous properties of the selected Zr-MOFs along with linker and molecular formulas. Representative structures of the two Zr-MOFs are shown in **Fig. S4**. UiO-66(Zr) and MOF-801 have the same metal center to linker co-ordination number (12), and almost similar porous properties.

However, MOF-808 with metal centers-to-linker co-ordination number "6"possesses porous properties different from other two Zr-MOFs (Table2 and **Fig.S5**). Anticipating pronounced potential of MOF-808 due to its large surface area and bigger pore size, it was decided to check the performance of the catalyst at moderate reaction temperature to represent the principle of green chemistry.

**Table 3** demonstrates the catalytic activity of various Zr-based catalysts at moderate reaction temperature. Three different MOFs were compared in terms of conversion, yield, GVL formation rate and turn-over frequency (TOF) (entry number 1– 3 in Table 3). Indeed, MOF-808 had an edge over the other two MOFs. The reason is quite clear, its greater surface area provides more active sites and its bigger pore size provides easy access to active sites. UiO-66(Zr) gives higher conversion (43.3%) than MOF-801 (28.1%) despite having the same window size (6 Å). This was probably due to higher external surface area (390 $m^2/g$ for UiO-66(Zr) and 168 $m^2/g$ for MOF-801) and pore volume. We have compared our results with $ZrO_2$, $ZrO(OH)_2$ and other Zr based catalysts reported in the literatures, studied under comparable reaction conditions

**Table 2** Linker, and molecular formulas and porous properties of Zr-MOFs.

| MOF | Linker | Molecular formula | $S_{BET}$[a] ($m^2/g$) | PV[b] ($cm^3/g$) | PD[c] (Å) |
|---|---|---|---|---|---|
| MOF-801 | Fumaric acid | $Zr_6O_4(OH)_4(fumarate)_6$ | 990 | 0.44 | 6 |
| UiO-66(Zr) | 1,4 Benzenedicar-boxylic acid (BDC) | $Zr_6O_4(OH)_4(BDC)_6$ | 1046 | 1.65 | 6 |
| MOF-808 | 1,3, 5 Benzenetri-carboxylic acid (BTC) | $Zr_6O_4(OH)_4(BTC)_2(HCOO)_6$ | 1450 | 0.8 | 7.4, 12.5 |

[a]$S_{BET}$ =BET surface area as a nominal surface area, [b]PV= Pore Volume, [c]PD= Pore Diameter

(entry 6 -8). MOF-808 was found superior in terms of GVL formation rate compared to all other catalysts mentioned in Table 3 under specific reaction conditions. Amorphous Zr-complexes were also showed good performance at lower temperature (entry 6, and 7), but they lagged behind MOF-808 in terms of GVL formation rate. This was ascribed to their low crystallinity or poorly ordered structure, which resulted to smaller surface area compared to highly ordered, crystalline MOF-808. Nevertheless, at higher temperature all the compared catalysts showed quantitative product yield. The porous properties of the catalysts mentioned in table 3 are reported in the supplementary information **Table S2**.

With such exceptional catalytic activity of MOF-808, we extended our approach to carry out this reaction in an open system using the solvent reflux method (entry 10). In organic synthesis, several reduction reactions have been practiced using homogeneous catalytic systems.[72-74] The moisture sensitivity, stoichiometric use and difficulties in the separation and reusability of the catalysts make homogeneous systems less efficient. Therefore, it is highly desirable to use heterogeneous catalyst to overcome the difficulties associated with homogeneous catalytic systems.[75-77] In return, catalyst must be active and selective toward targeted compounds under moderate reaction conditions. This is because pressurized reactions are out of consideration in organic synthesis due to the hazardous nature of several chemicals and related safety concerns. MOF-808 showed good performance in open system MPV reduction of EL at its boiling point, producing 75% GVL yield in 18 h. It should be noted that MOF-808 was still active in open system at milder reaction conditions and could be utilized in organic synthesis where most of the reactions are performed in open system at moderate reaction conditions.

However, when LA was used as precursor for the GVL production, MOF-808 has some limitations, which showed only 4.3% GVL yield due to strong binding ability of carboxylic group in LA to the basic metal sites of MOF-808 confirmed by FTIR and TG analysis

**Table 3** CTH of EL catalyzed by various catalysts at moderate reaction temperature

| Entry | Catalyst | Temp. (°C) | Time (h) | Conv. (%) | Yield (%) | Mass ratio catalyst :ester | GVL FR[f] (µmol/g/min) | TOF ($h^{-1}$) | Reference |
|---|---|---|---|---|---|---|---|---|---|
| 1 | MOF-808 | 130 | 3 | 100 | 85.0 | 1:2.9 | 94.4 | 7.7 | This study |
| 2 | UiO-66(Zr) | 130 | 3 | 43.3 | 8.0 | 1:2.9 | 8.9 | 0.8 | This study |
| 3 | MOF-801 | 130 | 3 | 28.1 | 12.2 | 1:2.9 | 13.6 | 1.1 | This study |
| 4 | $ZrO_2$ | 130 | 3 | 36.5 | 21.9 | 1:2.9 | 24.3 | 0.2 | This study |
| 5 | $ZrO(OH)_2$ | 130 | 3 | 50.5 | 33.7 | 1:2.9 | 37.4 | 0.3 | This study |
| 6 | Zr-HBA | 120 | 4 | 82.1 | 50.1 | 1:0.7 | 10.4 | 0.1 | 34 |
| 7 | Zr-PhyA | 130 | 8 | 98.9 | 95.4 | 1:0.7 | 9.9 | 0.7 | 39 |
| 8[b] | Zr-Beta | 118 | 22 | 88 | 83 | 1:1.2 | 6.3 | 3.7 | 42 |
| 9[c] | Zr-Beta | 82 | 18 | 5.6 | 4.0 | 1:0.6 | 0.2 | 0.1 | 42 |
| 10[d] | MOF-808 | 82 | 18 | 100 | 75 | 1:0.7 | 3.5 | 1.1 | This study |
| 11[e] | MOF-808 | 82 | 18 | 61.7 | 4.3 | 1:0.7 | 0.2 | 0.1 | This study |

[a] Reaction conditions: EL 4 mmol; isopropanol 400 mmol; catalyst 0.2 g; naphthalene 0.24 g; [b, c] Reactant was LA and 2-pentanol as hydrogen donor, for [c] Open system solvent reflux method was used; [d,e] Reaction carried out in open system (solvent reflux method) catalyst- 0.8g; [e] Reactant was LA; [f] GVL FR (formation rate) = (mole of GVL)/(amount of catalyst X reaction time). Turn-over frequency (TOF)= (mole of GVL)/(mole of active sites of catalyst X time)

of fresh and spent catalysts **(Fig S6)**. FTIR shows extra peaks (C=O stretch at 1715 $cm^{-1}$ and C-O stretch at 1165 $cm^{-1}$) in spent catalyst, TGA shows higher weight loss of spent catalyst in the temperature range of 350$^{O}$C to 550$^{O}$C attributed to LA bonding with MOF-808. Acid-base sites of Zr-MOFs are required for MPV reduction (explained thoroughly in mechanism part). Blocking these basic sites by strong adsorption of LA would be thus reflected as a decline in catalytic activity. This kind of inhibiting effect of LA in CTH reaction over $ZrO_2$ catalyst was reported previously. [35]

Effect of reaction temperature on catalytic activity of MOF-808 was studied at moderate temperatures (**see Fig.S7**). It was found that, at lower reaction temperature 110$^{O}$C catalyst produces around 64% GVL yield with IPL as major side product. MOF-808 showed its best performance at 130$^{O}$C with 85% GVL yield.

Furthermore, MOF-808 was recycled five times in a batch-type pressurized reaction system without notable change in catalytic activity **Fig S8**. Recycled catalyst was characterized in detail, using X-ray diffraction, $N_2$ physisorption, TGA, FTIR, and SEM analysis as shown in **Fig S9**. XRD patterns displayed no change in the crystal structure of used catalyst; all the peaks retained the same intensity. The BET surface area of the used catalyst decreased from the initial 1450 to 900 $m^2/g$. TGA and FTIR patterns further validated the structural changes that occurred in the catalyst after the fifth run. Weight loss in the temperature range of 375 to 700$^{o}$C assigned to the BTC ligand was almost identical in fresh and used catalyst, which confirmed no leaching of the BTC ligand from the structure. However, the main difference in weight loss occurred in the middle temperature range (175 to 375$^{o}$C) associated with OH and remnant formate group in the MOF-808 structure. Substantial reduction in OH stretching frequency in the FTIR pattern of used catalyst indicates the deviations in the OH group present in MOF-808. Additionally, no leaching of metal from MOF structure was confirmed by ICP analyses (Table S1). Hitherto, unlike UiO-66(Zr), it is difficult to propose the probable formula for MOF-808 using TG and elemental analysis due to overlapping of the degradation temperature range of OH and formate groups in the thermo-gravimetric analysis. In previous reports, formate groups were easily replaced by other groups and were considered the main sites for activation and functionalization of MOF-808.[78, 79] Morphological and X-ray diffraction study suggested that no phase transition or structure collapse occurred even after five recycle tests, and this observation is in line with the high chemical stability reported for MOF-808 in previous studies.[80] Further research is in progress to understand the structural changes after post synthetic modification of MOF-808. Once again, as with UiO-66(Zr), structural changes in MOF-808 did not affect the catalytic activity or product selectivity.

### 3.5 Reaction Mechanism

Earlier in this paper, we proved that ligand functionality (acid or base) was not really effective in selective transformation of alkyl levulinate into GVL, and instead decreased the catalytic activity. Furthermore, the results obtained from characterization of fresh and used catalyst also supported the fact that metal clusters/centers of the Zr-MOF framework were the active sites producing GVL from EL via CTH.

According to previous studies, the amphoteric nature of the catalysts was the major cause for their high activity in MPV reduction of EL to GVL.[35, 39] Therefore, Zr-MOFs (MOF-808 and UiO-66(Zr)) were subjected to $NH_3$-TPD and $CO_2$-TPD to determine their acid and base properties, respectively **(Fig S10).** The obtained results shows that both the Zr-MOFs possess acidic and basic sites; and that moreover, the quantity of these sites was much greater in MOF-808 than UiO-66(Zr). The origin of the acid-base sites was development from Zr-O-Zr or Zr-OH-Zr bonding present in the metal clusters of the Zr-MOFs, similar to the bonding observed in $ZrO_2$ and $Zr(OH)_4$. Considering all the above mentioned points, a plausible reaction mechanism for this reaction was proposed in **Scheme 2**. The combination of acid and base sites ($Zr^{4+}$ and $O^{2-}$) from the metal cluster interacted with both isopropanol and EL to form a six membered ring transition state.[35, 36, 37, 81] At this stage, corresponding alkoxide generated from the dissociation of isopropanol, readily transfered hydride ions to attack the carbonyl group of EL to yield 4-hydroxypentanoate (4-HPE). At the same time, isopropanol was converted into acetone with the loss of two hydrogen atoms. No detection of 4-HPE by GC analysis supported the fact that fast intramolecular transesterification of 4-HPE into GVL was accompanied by equimolar production of ethanol.[35, 37, 42] Liu et.al. thoroughly studied the pathway and mechanism for this reaction using $ZrO(OH)_2$.[37] Only two other major products were detected by GC-MS besides GVL. The first was IPL, a by-product formed by transesterification of EL, which underwent further CTH (like EL) to yield GVL. Another observed by-product was ethyl 4-isopropoxypentanoate (E4iPOPA), probably formed by etherification of 4-HPE with isopropanol. Formation of E4iPOPA could be considered another indirect evidence for the formation of 4-HPE. Several attempts have been made to produce these kinds of bio-oxygenates from GVL which considered as more suitable candidates for gasoline additives and diesel components than GVL itself. [82, 83]

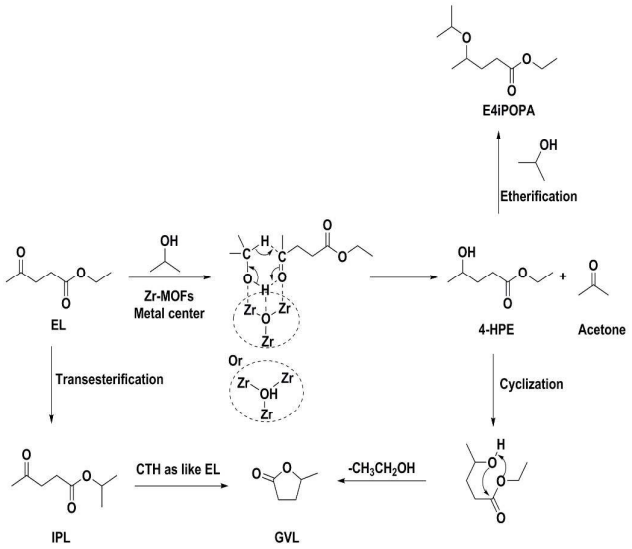


**Scheme 2** Plausible reaction mechanism for CTH of EL to GVL using Zr-MOFs

Finally, it has been proved that metal cluster in Zr-MOFs are the active sites in this reaction and that the unique ability of the Zr-MOFs to undergo structural rearrangement to stabilize its structure helped to maintain the catalyst activity and selectivity toward GVL. Higher surface area, pore size of Zr-MOFs and the accessibility of the reactant molecule to the metal center of MOFs play pivotal roles in achieving high GVL formation rate and turnover frequency under moderate reaction conditions.

**Conclusions**

In summary, a series of crystalline porous Zr-MOFs were synthesized and tested for CTH of EL via MPV reduction using isopropanol as hydrogen donor. The roles of the metal center and ligand functionality of UiO-66(Zr) were determined in order to understand the origin of the active sites. UiO-66(Zr) showed high chemical stability and catalytic activity at high temperature (200$^{o}$C). Therefore, it appears a good potential catalyst for high temperature reactions for biorefinery.

MOF-808, which has large surface area and a wide pore structure, proved to be highly effective for producing GVL from EL at moderate reaction temperature with high GVL formation rate (94.4 μmol/g/min). Moreover, it showed good performance in an open system using the solvent reflux method. Both UiO-66(Zr) and MOF-808 catalysts could be recycled at least five times under the specified reaction conditions without loss of catalytic activity. The Zr-MOFs have a unique property of being able to undergo structural rearrangement to stabilize the framework, which was proven using several characterization techniques. The probable reaction mechanism of this reaction over Zr-MOFs was proposed. The metal nodes that develop the acid-base properties in Zr-MOFs, are considered the active sites in selective formation of GVL from EL. Excellent performance by highly crystalline porous Zr-MOFs for transfer hydrogenation of EL at high and low temperature will pave the way for a detailed exploration of these catalysts for the MPV reduction of various substrates in biorefinery and organic synthesis.

## Acknowledgements

This work was supported by the R&D Program of the Institutional Research Program of KRICT [KK1601-C100], and partly by the Agency of Defense Development of Korea (UE1351521D). JSC is kindly grateful to the National Research Council of Science and Technology (NST) for financial support. Authors thank Prof. Y. -S. Bae for his beneficial contribution.

## Notes and references

1 G. W. Huber and A. Corma, *Angew. Chem. In. Ed.*, 2007, **46**, 7184.
2 A. J. Ragauskas, C. K. Williams, B. H. Davison, G. Britovsek, J. Cairney, C. A. Eckert, W. J. Frederick, J. P. Hallett, D. J. Leak, C. L. Liotta, J. R. Mielenz, R. Murphy, R. Templer and T. Tschaplinski, *Science*, 2006, **311**, 484.
3 P. P. Upare, D. W. Hwang, Y. K. Hwang, U. H. Lee, D.-Y. Hong and J.-S. Chang, *Green Chem.*, 2015, **17**, 3310.
4 A. Osatiashtiani, A. F. Lee, M. Granollers, D. R. Brown, L. Olivi, G. Morales, J. A. Melero and K. Wilson, *ACS Catal.*, 2015, **5**, 4345.
5 R. Weingarten, W. C. Conner and G. W. Huber, *Energy Environ. Sci.*, 2012, **5**, 7559.
6 P. P. Upare, J.-W. Yoon, M. Y. Kim, H.-Y. Kang, D. W. Hwang, Y. K. Hwang, H. H. Kung and J.-S. Chang, *Green Chem.*, 2013, **15**, 2935.
7 M. S. Holm, S. Saravanamurugan and E. Taarning, *Science*, 2010, **328**, 602.
8 A. Fukuoka and P. L. Dhepe, *Angew. Chem.*, 2006, **118**, 5285.
9 J. Q. Bond, D. M. Alonso, D. Wang, R. M. West and J. A. Dumesic, *Science*, 2010, **327**, 1110.
10 D. M. Alonso, S. G. Wettstein and J. A. Dumesic, *Green Chem.*, 2013, **15**, 584.
11 W. Luo, M. Sankar, A. M. Beale, Q. He, C. J. Kiely, P. C. Bruijnincx and B. M. Weckhuysen, *Nat. Commun.*, 2015, **6**, 6540.
12 J. P. Lange, R. Price, P. M. Ayoub, J. Louis, L. Petrus, L. Clarke and H. Gosselink, *Angew. Chem. In. Ed.*, 2010, **49**, 4479.
13 J. Q. Bond, A. A. Upadhye, H. Olcay, G. A. Tompsett, J. Jae, R. Xing, D. M. Alonso, D. Wang, T. Zhang, R. Kumar, A. Foster, S. M. Sen, C. T. Maravelias, R. Malina, S. R. H. Barrett, R. Lobo, C. E. Wyman, J. A. Dumesic and G. W. Huber, *Energy Environ. Sci.*, 2014, **7**, 1500.
14 J. P. Lange, J. Z. Vestering and R. J. Haan, *Chem Commun.*, 2007, 3488.
15 S. Raoufmoghaddam, M. T. Rood, F. K. Buijze, E. Drent and E. Bouwman, *ChemSusChem*, 2014, **7**, 1984.
16 P. P. Upare, J. M. Lee, Y. K. Hwang, D. W. Hwang, J. H. Lee, S. B. Halligudi, J. S. Hwang and J.-S. Chang, *ChemSusChem*, 2011, **4**, 1749.
17 T. Pan, J. Deng, Q. Xu, Y. Xu, Q.-X. Guo and Y. Fu, *Green Chem.*, 2013, **15**, 2967.
18 I. T. Horvath, H. Mehdi, V. Fabos, L. Bodaab and L. T. Mika, *Green Chem.*, 2008,**10**, 238.
19 E. I. Gurbuz, J. M. Gallo, D. M. Alonso, S. G. Wettstein, W. Y. Lim and J. A. Dumesic, *Angew. Chem.Int. Ed.*, 2013, **52**, 1270.
20 L. Qi and I. T. Horváth, *ACS Catal.*, 2012, **2**, 2247.
21 X. Tang, X. Zeng, Z. Li, L. Hu, Y. Sun, S. Liu, T. Lei and L. Lin, *Renewable and Sustainable Energy Rev.*, 2014, **40**, 608.
22 L. E. Manzer, *Appl. Catal. A*, 2004, **272**, 249.
23 P. P. Upare, J.-M. Lee, D. W. Hwang, S. B. Halligudi, Y. K. Hwang and J.-S. Chang, *J. Ind. Eng. Chem.*, 2011, **17**, 287.
24 A. M. Hengne and C. V. Rode, *Green Chem.*, 2012, **14**, 1064.
25 K.-i. Shimizu, S. Kanno and K. Kon, *Green Chem.*, 2014, **16**, 3899.
26 H. Zhou, J. Song, H. Fan, B. Zhang, Y. Yang, J. Hu, Q. Zhu and B. Han, *Green Chem.*, 2014, **16**, 3870.
27 L. E. Manzer, *Applied Catal. A,* 2004, **272**, 249.
28 E. F. Mai, M. A. Machado, T. E. Davies, J. A. Lopez-Sanchez and V. T. Silva, *Green Chem.*, 2014, **16**, 4092.
29 D. J. Braden, C. A. Henao, J. Heltzel, C. C. Maravelias and J. A. Dumesic, *Green Chem.*, 2011, **13**, 1755.
30 X.-L. Du, L. He, S. Zhao, Y.-M. Liu, Y. Cao, H.-Y. He and K.-N. Fan, *Angew. Chem. Int. Ed.*, 2011, **50**, 7815.
31 L. Deng, Y. Zhao, J. Li, Y. Fu, B. Liao and Q.-X. Guo, *ChemSusChem*, 2010, **3**, 1172.
32 P. P. Upare, M.-G. Jeong, Y. K. Hwang, D. H. Kim, Y. D. Kim, D. W. Hwang, U. H. Lee and J.-S. Chang, *Appl. Catal. A*, 2015, **491**, 127.
33 A. M. Hengne, A. V. Malawadkar, N. S. Biradar and C. V. Rode, *RSC Adv.*, 2014, **4**, 9730.
34 J. Song, L. Wu, B. Zhou, H. Zhou, H. Fan, Y. Yang, Q. Meng and B. Han, *Green Chem.*, 2015, **17**, 1626.
35 M. Chia and J. A. Dumesic, *Chem. Commun.*, 2011, **47**, 12233.
36 X. Tang, L. Hu, Y. Sun, G. Zhao, W. Hao and L. Lin, *RSC Adv.*, 2013, **3**, 10277.

37 X. Tang, H. Chen, L. Hu, W. Hao, Y. Sun, X. Zeng, L. Lin and S. Liu, *Applied Catal. B*, 2014, **147**, 827.
38 J. He, H. Li, Y.-M. Lu, Y.-X. Liu, Z.-B. Wu, D.-Y. Hu and S. Yang, *Applied Catal. A,* 2016, **510**, 11.
39 J. Song, B. Zhou, H. Zhou, L. Wu, Q. Meng, Z. Liu and B. Han, *Angew. Chem. Int. Ed.*, 2015, **54**, 9399.
40 S. S. Enumula, V. R. B. Gurram, M. Kondeboina,D. R. Burri and S. R. R. Kamaraju, *RSC Adv.,* 2016, **6**, 202326.
41 M. G. Al-Shaal, M. Calin, I. Delidovich and R. Palkovits, *Catal. Commun.*, 2016, **75**, 65.
42 J. Wang, S. Jaenicke and G.-K. Chuah, *RSC Adv.*, 2014, **4**, 13481.
43 L. Bui, H. Luo, W. R. Gunther and Y. Roman-Leshkov, *Angew. Chem. Int. Ed.*, 2013, **52**, 8022.
44 J. Gascon, A. Corma, F. Kapteijn and F. X. Llabrés i Xamena, *ACS Catal.*, 2014, **4**, 361.
45 M. Ranocchiari and J. A. van Bokhoven, *Phys. Chem. Chem. Phys.*, 2011, **13**, 6388.
46 D.-Y. Hong, Y. K. Hwang, C. Serre, G. Ferey and J.-S. Chang, *Adv. Funct. Mater.*, 2009, **19**, 1537.
47 G. Ferey, *Chem. Soc. Rev.*, 2008, **37**, 191.
48 E. S. Sanil, K. H. Cho, D.-Y. Hong, J. S. Lee, S. K. Lee, S. G. Ryu, H.-W. Lee, J.-S. Chang and Y. K. Hwang, *Chem Commun.*, 2015, **51**, 8418.
49 J. H. Cavka, S. Jakobsen, U. Olsbye, N. Guillou, C. Lamberti, S. Bordiga and K. P. Lillerud, *J. Am. Chem. Soc.*, 2008, **130**, 13850.
50 W. Liang, H. Chevreau, F. Ragon, P. D. Southon, V. K. Peterson and D. M. D'Alessandro, *CrystEngComm*, 2014, **16**, 6530.
51 G. E. Cmarik, M. Kim, S. M. Cohen and K. S. Walton, *Langmuir*, 2012, **28**, 15606.
52 H. Furukawa, F. Gandara, Y. B. Zhang, J. Jiang, W. L. Queen, M. R. Hudson and O. M. Yaghi, *J. Am. Chem. Soc.*, 2014, **136**, 4369.
53 T. Duerinck, R. Bueno-Perez, F. Vermoortele, D. E. De Vos, S. Calero, G. V. Baron and J. F. M. Denayer, *J. Phys. Chem. C,* 2013, **117**, 12567.
54 H. T. Zhang, J. W. Zhang, G. Huang, Z. Y. Du and H. L. Jiang, *Chem Commun.*, 2014, **50**, 12069.
55 F. Vermoortele, M. Vandichel, B. Van de Voorde, R. Ameloot, M. Waroquier, V. Van Speybroeck and D. E. De Vos, *Angew. Chem. Int. Ed.*, 2012, **51**, 4887.
56 F. Ragon, P. Horcajada, H. Chevreau, Y. K. Hwang, U.-H. Lee, S. R. Miller, T. Devic, J.-S. Chang and C. Serre, *Inorg. Chem.*, 2014, **53**, 2491.
57 G. Zahn, H. A. Schulze, J. Lippke , S. Konig , U. Sazama , M. Froba and P. Behrens, *Micropor. Mesopor. Mat.*, 2015, **203**, 186.
58 M. Kandiah, M. H. Nilsen, S. Usseglio, S. Jakobsen, U. Olsbye, M. Tilset, C. Larabi, E. A. Quadrelli, F. Bonino and K. P. Lillerud, *Chem. Mater.*, 2010, **22**, 6632.
59 F. Vermoortele, R. Ameloot, A. Vimont, C. Serre and D. D. Vos, *Chem. Commun.,* 2011, **47**, 1521.
60 F. Ragon, B. Campo, Q. Yang, C. Martineau, A. D. Wiersum, A. Lago, V. Guillerm, C.Hemsley, J. F. Eubank, M. Vishnuvarthan, F. Taulelle, P. Horcajada, A. Vimont, P. L. Llewellyn, M. Daturi, S. Devautour-Vinot, G. Maurin, C. Serre, T. Devic and G. Clet, *J. Mater. Chem. A*, 2015, **3**, 3294.
61 H. Jasuja, G. W. Peterson, J. B. Decoste, M. A.Browe and K. S. Walton, *Chem. Eng. Sci.*, 2015, **124**, 118.
62 S. Saravanamurugan, Sujandi, D.-S. Han, J.-B. Koo and S.-E. Park, *Catal. Commun.*, 2008, **9**, 158.
63 V. V. Guerrero and D. F. Shantz, *Ind. Eng. Chem. Res.,* 2009, **48**, 10375.
64 A. Villa, J.-P. Tessonnier, O. Majoulet, D. S. Su and R. Schlogl, *Chem. Commun.*, 2009, 4405.
65 M. Vandichel, J. Hajek, F. Vermoortele, M. Waroquier, D. E. D. Vos and V. V. Speybroeck, *CrystEngComm.*, 2015 , **17**, 395.
66 J. B. DeCoste, G. W. Peterson, H. Jasuja, T. G. Glover, Y. Huang and K. S. Walton, *J. Mater. Chem. A*, 2013, **1**, 5642.
67 J. D. Lewis, S. V. Vyver, A. J. Crisci, W. R. Gunther, V. K. Michaelis, R. G. Griffin and Y. Roman-Leshkov, *ChemSusChem*, 2014, **7**, 2255.
68 F. Vermoortele, B. Bueken, G. L. Bars, B. V. Voorde, M. Vandichel, K. Houthoofd, A. Vimont, M. Daturi, M. Waroquier, V. V. Speybroeck, C. Kirschhock and D. E. D. Vos, *J. Am. Chem. Soc.* 2013, **135**, 11465.
69 O. V. Gutov, M. G. Hevia, E. C. Escudero-Adán and A. Shafir, *Inorg. Chem.*, 2015, **54** , 8396.
70 L. Valenzano, B. Civalleri, S. Chavan, S. Bordiga, M. H. Nilsen, S. Jakobsen, K. P. Lillerud and C. Lamberti, *Chem. Mater*, 2011, **23**, 1700.
71 C. Larabi, and E. A. Quadrelli, *Eur. J. Inorg. Chem.* 2012, 3014.
72 C.F. de Graauw, J. A. Peters, H. van Bekkum and J. Huskens, *Synthesis*, 1994, **10**, 1007.
73 T Ooi, T. Miura and K. Maruoka, *Angew. Chem. Int. Ed.* 1998, **37**, 2347.
74 Y. Ishii, T. Nakano, A. Inada, Y. Kishigami, K. Sakurai and M. Ogawa, *J. Org. Chem.*, 1986, 51, 240.
75 J. R. Ruiz, C. Jimenez-Sanchidrian, J. M. Hidalgo and J. M. Marinas, *J. Mol. Catal. A: Chem.*, 2006, **246**, 190.
76 Y. Zhu, S. Jaenicke and G.K. Chuah, *J. Catal.*, 2003, **218**, 396.
77 R. Anwander, C. Palm, G. Gerstberger, O. Groeger and G. Engelhardt, *Chem. Commun.*, 1998, 1811.
78 S.-Y. Moon, Y. Liu, J. T. Hupp and O. K. Farha, *Angew. Chem. Int. Ed.*, 2015, **54**, 6795.
79 J. Jiang, F. Gandara, Y.-B. Zhang, K. Na, O. M. Yaghi, and W. G. Klemperer, *J. Am. Chem. Soc.* 2014, **136**, 12844.
80 W. Liang, H. Chevreau, F. Ragon, P. D. Southon, V. K. Peterson and D. M. DAlessandro, Cryst EngComm, 2014, **16**, 6530.
81 R Cohen, C. R. Graves, S. T. Nguyen, J. M. L. Martin and M. A. Ratner, *J. Am. Chem. Soc.* 2004, 126, 14796.
82 D. Fegyverneki, L. Orha, G. Lang and I.T. Horvath, *Tetrahedron*, 2010, **66**, 1078.
83 C. E. Chan-Thaw, M. Marelli, R. Psaro, N. Ravasio and F. Zaccheria, *RSC Adv.*, 2013, **3**, 1302.